

# A Novel Improvement of the Performance Coefficient of a Residential Air Source Heat Pump Water Heater

Stephen Tangwe, Kanzumba Kusakana

Central University of Technology, Free State, Bloemfontein, South Africa,

Email: lstephen@cut.ac.za; kkusakana@cut.ac.za

**Abstract** - Air Source Heat Pump (ASHP) water heaters are energy efficient and renewable energy devices employed for sanitary hot heating. The study focused on demonstrating that the Coefficient Of Performance (COP) of an ASHP unit are often higher than the COP of the ASHP water heater. The setup involved the design and installation of a 1.2 kW, 150 L ASHP water heater and a Data Acquisition System (DAS). The DAS consist of a power meter, flow meters, temperature sensors, pressure sensors, ambient temperature and relative humidity sensor and were installed at precise locations of the ASHP water heater. Specific controlled volume of 150, 50 and 100 L were drawn off from the ASHP water heater during the morning, afternoon and evening for a full year. The results depicted that during the summer and winter periods, the average COP of the ASHP water heater was 3.04 and 2.32, respectively. On the contrary, the COP of the ASHP unit was 3.53 and 2.99, respectively. The implementation of electric motors in the prime movers (fan, pump and compressor) with better energy efficiency to replace the existing electric motors, can enhanced the COPs of the ASHP unit and the ASHP water heater.

**Keywords** - Air source heat pump (ASHP) water heater, Coefficient of performance (COP), COP of ASHP unit (COPt), COP of ASHP water heater (COPE), Renewable energy device, Data acquisition system

## I. INTRODUCTION

Sanitary hot water heating is among the residential processes associated with huge electrical energy consumption [1]. In South Africa, sanitary hot water heating contributed between 30 and 50% of the monthly electrical energy cost and the majority of the hot water heating is achieved through the inefficient geysers [2]. Geysers are often retrofitted with ASHP units and the resultant device is called ASHP water heaters. The special characteristic that gives the excellent performance of the ASHP water heaters is known as the Coefficient Of Performance (COP) and the device is considered as a renewable and an energy efficient technology [3, 4]. The COP of the ASHP water heater ranges from 2 to 4 and it depends on the ambient temperature, the system design and the hot water heating loads [5, 6, 7]. The operational performance of the ASHP water heaters has been reported to be better in the summer than in the winter periods. This can be accounted by the favorable ambient temperature experienced during the summer [8]. The ASHP water heaters are commonly divided into the split and integrated types. In the split type ASHP water heater, the ASHP unit and the hot water storage tank are connected by copper pipes with the ASHP unit situated below the tank. Conversely, the integrated type ASHP water heater is a compact design with the ASHP unit situated above the tank while the condenser is immersed into the tank [10]. The prime movers of a typical ASHP water heater includes the compressor, the fan and the water circulation pump. Extensive research conducted have shown that the integrated type ASHP water heaters performed

better than the split type ASHP water heaters, provided they are of the same input electrical power and tank size (both types are without auxiliary electric backup) [11, 12]. Furthermore, the integrated type ASHP water heater is very unstable and experiences lower standby losses, unlike the split type ASHP water heater [13]. Although, the ASHP water heaters are efficient hot water heating devices, the COP can further be improved, if the ASHP water heater is forced to operate within the range of the COP of the ASHP unit [14]. The study focused on the investigation and analyses of the input electrical and the useful output thermal energy gain by the ASHP water heater due to specific volume of hot water drawn off. And it also deal with the determination of the change in enthalpy of the refrigerant at the inlet and outlet of the heat exchangers (evaporator and condenser) of the ASHP unit, due to the specific volume (50, 100 and 150 L) of hot water drawn off.

For full list of Nomenclature see Appendix.

## II. FUNDAMENTALS OF THE HEAT PUMP OPERATIONS

An ideal ASHP water heater transfers thermal energy during its vapor compression refrigeration cycle (VCRC) from the ambient air to heat water in the storage tank. The process may lead to cooling and dehumidification of the air to a certain degree based on the ambient condition. Figure 1 provides a schematic diagram of the components that are involved in the VCRC occurring in a typical ASHP water heater. A salient and better understanding of the refrigeration cycle of the heat pump water heater was given

by Ashdown (2004) and Sinha and Dysarkar (2008) [15, 16]. During a VCRC, aero-thermal energy gained by the evaporator is absorbed via the refrigerant R417A (liquid and vapour coexist) to change the phase of the liquid portion to vapour (latent heat) and also, the refrigerant gain sensible thermal energy. The process is relatively isobaric and occurs at phase (4 - 1) as shown in Figures 2 and 3. The difference in pressure between the suction and the discharge end, enables the refrigerant vapour (dry and low temperature and pressure refrigerant vapour) to flow to the compressor. In the compressor, the vapour is being compressed to a super-heated vapour and exits along the discharge line. The process is described as isentropic and occurs at phase (1 - 2) as illustrated in Figures II and III. As the super-heated refrigerant vapour flows into the condenser, the refrigerant is condensed, and a saturated refrigerant liquid is formed. The thermal energy dissipated is used to heat the water flowing through the inner tube of the condenser. During the phase (2 - 3) as shown in

Figures II and III, the temperature of the super-heated vapour drops, resulting in the formation of a sub-cool vapour, which in turn loses thermal energy to become a saturated refrigerant liquid. The process is referred to as isobaric condensation. At the expansion valve, the pressure and the temperature decrease and the saturated refrigerant liquid become a low-pressure liquid refrigerant. The process is an isenthalpic process and occurs at phase (3 - 4) as presented in Figures II and III. The ASHP water heater is capable to transport thermal energy from the air (cold reservoir) to heat water (hot reservoir) and this process is feasible, due to the input of energy (electrical) into the heat pump (cyclic engine). This is in accordance with the Clausius's statement derived from the second law of thermodynamics [17]. An efficiently installed ASHP water heater has a COP ranging from 2 to 4, whereas typical conventional water heaters (i.e. electric resistance element, coal, gas, kerosene stove, etc.) have a performance energy factor that is less than or equal to 1 [18, 19].

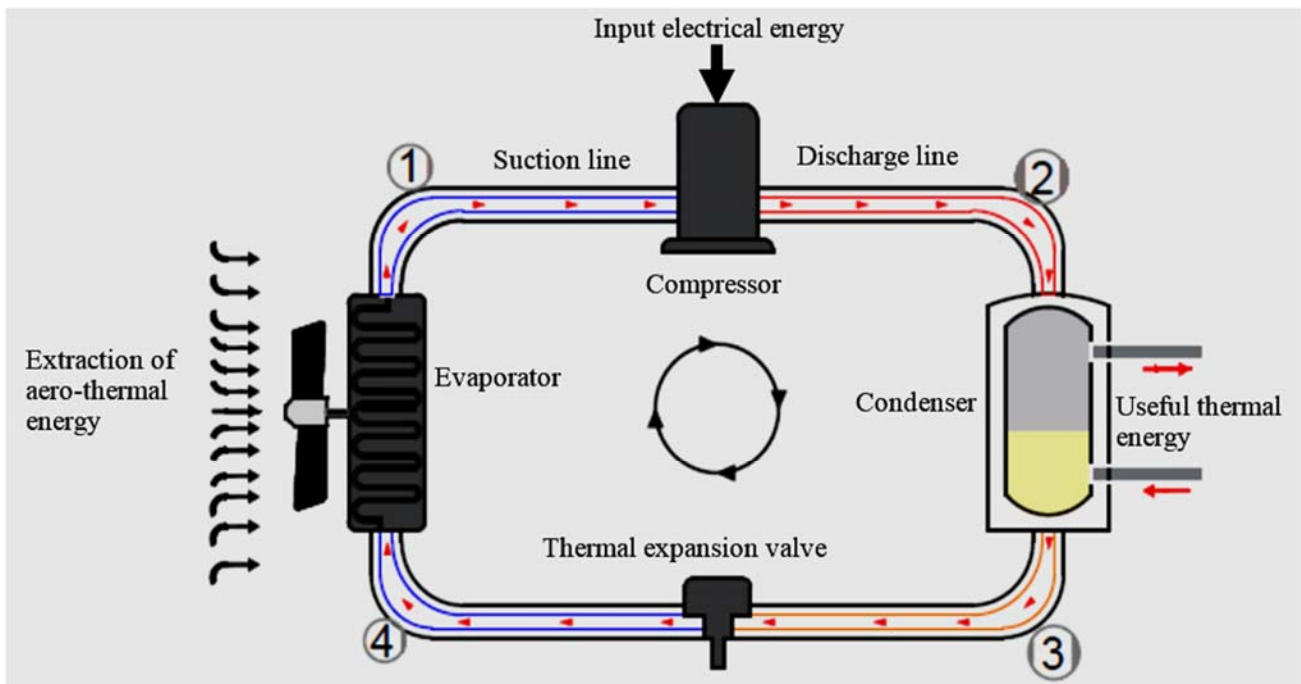


Figure 1. A schematic block diagram of the main components of an ASHP

Figure 2 shows the temperature versus entropy (T-S) graph for the VCRC of the ASHP water heater using the refrigerant R417A. The process occurring between phase 4-1 is known as isobaric evaporation and temperature glide is exhibited at the evaporator. The process occurring between phase 2-3 is known as isobaric condensation and there exist temperature glide at the condenser.

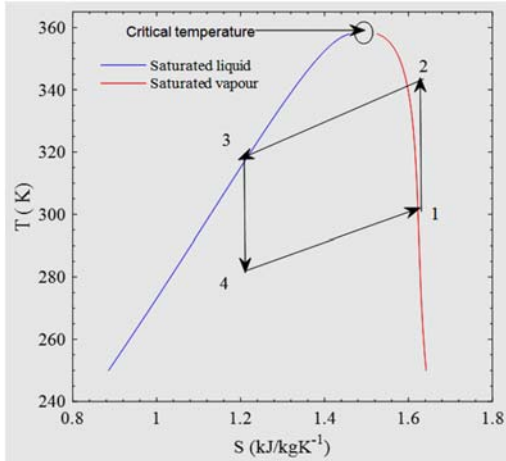


Figure 2. T-S graph of the VCRC in ASHP water heater using R417A

Figure 3 shows the pressure versus enthalpy (P-h) graph of the VCRC of the ASHP water heater using the refrigerant R417A. The process occurring between the phase 4-1 is known as isobaric evaporation and a constant pressure was experienced at the evaporator. The process occurring between the phase 2-3 is known as isobaric condensation and the pressure is constant throughout the condenser.

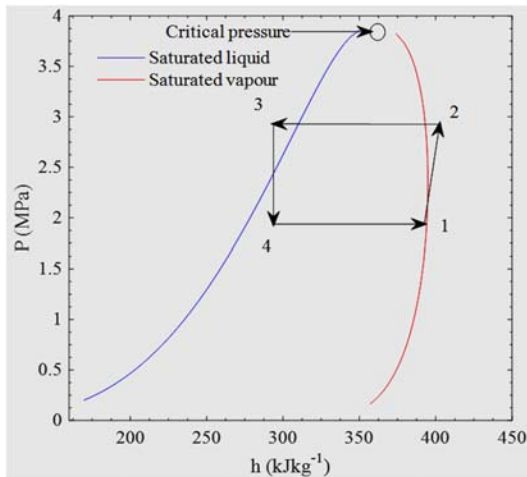


Figure 3. P-h graph of the VCRC in ASHP water heater using R417A

### III. CALCULATION AND THEORY

The input electrical energy consumed by the ASHP water heater during a VCRC is the product of the average electrical power consumed and the time taken, given in Equation 1.

$$EE = pt \tag{1}$$

The useful output thermal energy gained by the stored hot water is the product of the mass of water heated by the ASHP unit, the specific heat capacity of water and the difference in the water temperature between the outlet and inlet of the ASHP unit, during the VCRC given in Equation 2.

$$TE = mc(T_o - T_i) \tag{2}$$

The COP of the ASHP water heater with respect to the input and output energies, is defined as the ratio of the useful output thermal energy gained by the stored water and the input electrical energy consumed during the VCRC given in Equation 3.

$$COP_e = \frac{TE}{EE} \tag{3}$$

The COP of the ASHP unit relating to the changes in enthalpies is defined as the ratio of the change in the enthalpy of the refrigerant at the inlet and the outlet of the condenser to the difference between the change in the enthalpy of the refrigerant at the inlet and outlet of the condenser and the evaporator during the VCRC. The relationship is explicitly shown in Equation 4:

$$COP_t = \frac{h_{coni} - h_{cono}}{(h_{coni} - h_{cono}) - (h_{evpo} - h_{evpi})} \tag{4}$$

## IV. MATERIALS AND METHODS

### A. Materials

The list of materials used in the study are presented in Table I.

TABLE I. LIST OF MATERIALS EMPLOYED IN THE STUDY

Item	Material	Quantity
1	1.2 kW split type ASHP unit (1 Phase, 240 V, 50 Hz, R417A)	1
2	150 L, 3 kW high pressure geyser	1
3	Hot water volume control valve	1
4	Ambient temperature and relative humidity sensor	1
5	Power meter	1
6	Temperature sensors	11
7	Pressure sensors	4
8	Flow meters	2
9	Hot water collecting drum	1
10	Data loggers	2
11	REFPROP software	1
12	Hoboware pro software	1
13	Weather and waterproof enclosure	1

### B. Methods

The methods implemented for the study were divided into four procedures as follows:

The design and installation of the split type ASHP water heater and the configuration and installation of the sensors.

The conduction of the hot water drawn off (50, 100 and 150 L) during the time of use for both the summer and winter periods.

Analysis of the COP of the ASHP water heater for both the summer and winter periods in terms of the input electrical energy consumed and the useful output thermal energy gained due to the specific volumes (50, 100 and 150 L) of hot water drawn off.

Analysis of the COP of the ASHP unit for both the summer and winter periods pertaining to the enthalpy change between the inlet and outlet of the evaporator and condenser as a result of the specific volumes (50, 100 and 150 L) of hot water drawn off.

### C. Experimental Setup

Figure 4 shows the schematic diagram of the installed split type ASHP water heater at the outdoor space of the renewable energy laboratory, at the Central University of Technology, Free State Province, South Africa. The split type ASHP water heater comprised of a 1.2 kW input ASHP unit (single phase system with refrigerant R417A) and a 150 L, 3kW geyser. The geyser served as a storage tank with its 3 kW heating element disabled while retrofitted by the ASHP unit. The ASHP unit was positioned below the geyser and both devices were connected by reticulation copper pipes as shown in Figure IV. The ASHP unit was embedded with a 90 W water circulation pump that provided the require water pressure. The pressure exerted by the pump allow for the circulation of water between the geyser and the ASHP's condenser during the VCRC. The ASHP unit contained a propeller axial fan of 70 W, at the rear end of the evaporator. The fan assist in the creation of a force convection of the ambient air in the vicinity of the ASHP unit. The force convection process helped in accelerating the extraction of aero-thermal energy into the refrigerant at the evaporator during the VCRC.

Figure 5 shows the schematic layout of the split type ASHP water heater and the installed sensors. An ambient temperature and relative humidity sensor (Ta/RH) was installed in the vicinity of the split type ASHP water heater and measured both the ambient temperature and relative humidity. A power meter with an inbuilt logging capability

was installed on the power line supplying electricity to the split type ASHP unit and measured the input electrical power consumed by the ASHP water heater. Two flow meters (V and Vd) were installed closed to the inlet of the ASHP unit and at a position on the copper pipe, in proximity to the hot water discharge end of the geyser. The flow meters measured the volume of hot water heated by the ASHP unit and the volume of hot water drawn off from the storage tank, respectively. Eleven temperature sensors were installed at different locations on the installed ASHP water heater. Temperature sensor (T1) measured the temperature of the incoming cold water from the mains into the storage tank of the ASHP water heater. Temperature sensor (T2) measured the temperature of the air in the vicinity of the ASHP's evaporator. Temperature sensor (T3) measured the temperature of the hot water discharged from the storage tank into the collecting drum. Temperature sensors (T4 and T5) measured the temperature of the water at the inlet and the outlet of the ASHP unit. Temperature sensors (T6 and T7) measured the temperature of the refrigerant at the suction and discharge ends of the ASHP's compressor. Temperature sensors (T8 and T9) measured the temperature of the refrigerant at the inlet and the outlet of the ASHP's condenser. Finally, the temperature sensors (T10 and T11) measured the temperature of the refrigerant at the outlet and the inlet of the ASHP's evaporator. The pressure transducers (P1 and P2) measured the pressure of the refrigerant at the inlet and the outlet of the ASHP's evaporator. The pressure transducers (P3 and P4), measured the pressure of the refrigerant at the inlet and the outlet of the ASHP's condenser. All the sensors and the transducers were accommodated in two U30 no remote communication data loggers and each comprised of 15 logging channels. All the sensors and transducers were products of the Hobo Corporation and were compatible with the U30 no remote communication data loggers. The sensors and transducers were configured by the hoboware Pro software to log in 5-minute interval throughout the experiment. The data acquisition system was housed in a waterproof enclosure to prevent it from being damaged by interference from solar radiations and other unfavorable ambient conditions. The enthalpy measurements were obtained from the REFPROP upon running of the simulation of the saturated liquid and vapour table for the refrigerant R417A. The generated saturated refrigerant table was based on both the measured temperatures and pressures of the refrigerant (R417A) at the inlet and the outlet of the evaporator and the condenser during the VCRC [20, 21].

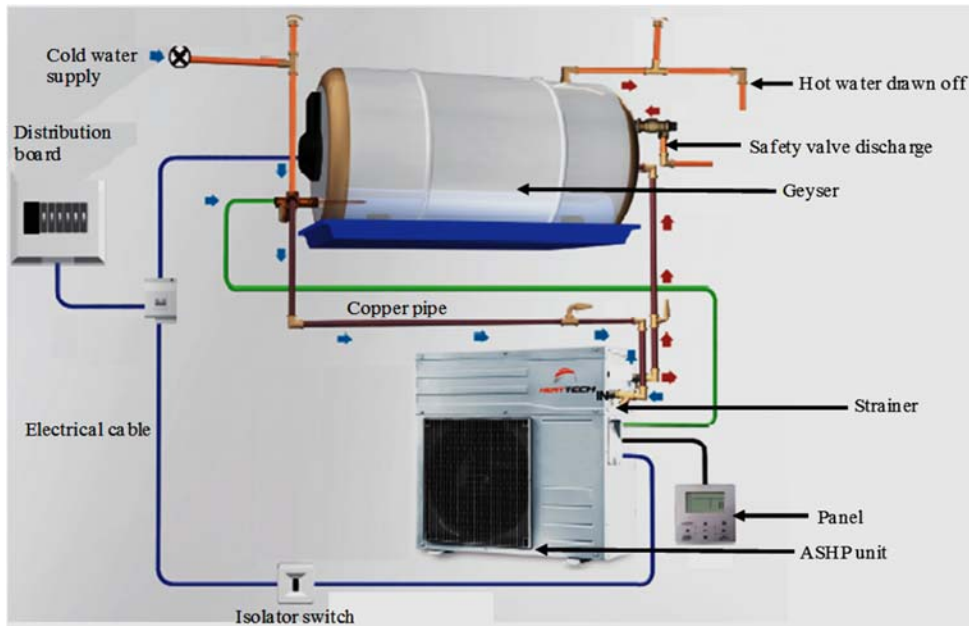


Figure 4. Schematic diagram of the installed split type ASHP water heater

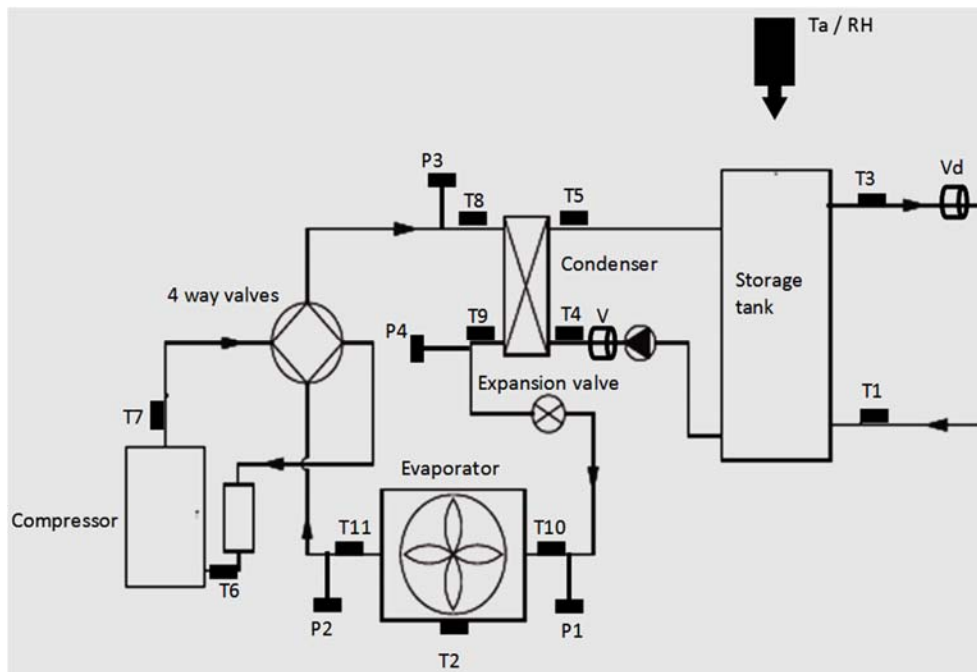


Figure 5. Schematic layout of the installed split type ASHP water heater and the sensors

## V. RESULTS AND DISCUSSION

### A. COP as function of energies and the impact of refrigerant temperatures

The temperatures of the refrigerant at the inlet and the outlet of the evaporator and the condenser of the ASHP unit, the input power consumed, the electrical energy consumed,

the thermal energy gained and the derived energies dependent coefficient of performance (COPE) of the ASHP water heater were analyzed for the summer (January to March 2018 and October to December 2018) and the winter (April to July 2018) periods after 50, 100 and 150 L hot water drawn off from the storage tank of the ASHP water heater.

### A1. Summer Performance of the COPE and Impact of the Refrigerant Temperatures

Table II shows the minimum, the maximum and the average temperatures of the refrigerant at the inlet and the outlet of the evaporator and the condenser, the electrical power consumed, the electrical energy consumed, the thermal energy gained and the derived COPE during the VCRC, due to 50, 100 and 150 L of hot water drawn off. It can be depicted from Table II that the temperature of the refrigerant at the inlet of the evaporator was lower (with an average of 4 oC) compared to the temperature of the refrigerant at the outlet of the evaporator (with an average of 27 oC) in all the drawn off scenarios. The difference between the temperature of the refrigerant at the outlet and the inlet of the evaporator showed that both sensible and latent heat were gained by the refrigerant at the evaporator during the VCRC. The temperature of the refrigerant at the

inlet of the condenser was higher (average of 79 oC) than the temperature of the refrigerant at the outlet of the condenser (average of 39 oC). The difference in the temperature of the refrigerant between the inlet and the outlet of the condenser depicted that thermal energy was dissipated from the refrigerant at the condenser during the VCRC. The useful output thermal energy was the portion of the dissipated energy that was absorbed by the stored water, enabling it to attain the set point temperature during the VCRC. The power consumed throughout the heating cycle, showed no significant difference over the different volumes of hot water drawn off and the average was 1.27 kW. However, both the electrical energy consumed and the useful thermal energy gained demonstrated a significant difference between the 50 L drawn off (1.01 and 3.03 kWh) to either the 100 or 150 L drawn off (1.55 and 4.66 kWh; 1.51 and 4.61 kWh). The average COPE for the different volumes of hot water drawn off was 3.02.

TABLE II. SUMMER POWER, TEMPERATURES AND COPE WITH RESPECT TO SPECIFIC VOLUMES OF DRAWN OFF

Parameters	50 L drawn off recorded parameter values			100 L drawn off recorded parameter values			150 L drawn off recorded parameter values		
	Min	Max	Average	Min	Max	Average	Min	Max	Average
Tevpi / °C	4.02	7.03	4.93	4.94	3.93	3.82	2.81	5.11	4.07
Tevpo / °C	22.83	36.56	27.47	22.31	27.26	24.90	21.32	34.29	27.76
Tconi / °C	65.50	82.50	74.72	74.54	78.84	76.42	73.77	84.03	79.54
Tcono / °C	38.16	45.22	42.05	38.43	39.69	39.00	36.95	42.51	39.97
p / kW	1.12	1.30	1.21	1.24	1.29	1.27	1.25	1.32	1.29
EE / kWh	0.98	1.03	1.01	1.51	1.55	1.55	1.43	1.67	1.51
TE / kWh	2.94	3.20	3.03	4.75	4.54	4.65	4.28	5.16	4.61
COPE	3.01	3.12	3.00	3.02	3.07	3.00	2.99	3.10	3.07

Tevpi = Refrigerant temperature at inlet of evaporator, Tevpo = Refrigerant temperature at outlet of evaporator, Tconi = Refrigerant temperature at inlet of condenser, Tcono = Refrigerant temperature at outlet of condenser, P = average power consumed, EE = Electrical energy consumed, TE = Thermal energy consumed, COPE = Energy dependent COP

### A2. Winter Performance of the Cope and Impact of the Refrigerant Temperatures

Table III presents the minimum, the maximum and the average temperatures of the refrigerant at the inlet and the outlet of the evaporator and the condenser, the electrical power consumed, the electrical energy consumed, the thermal energy gained and the derived COPE during the VCRC, due to 50, 100 and 150 L of hot water drawn off. The temperature of the refrigerant at the inlet of the evaporator was lower (with an average of 4 oC) relative to the temperature of the refrigerant at the outlet of the evaporator (with an average of 21 oC) throughout the different drawn off scenarios. The temperature of the refrigerant at the inlet of the condenser (with an average of 70 oC ) was higher as compared to the temperature of the refrigerant at the outlet of the condenser (37 oC). The

difference in the temperatures of the refrigerant between the inlet and the outlet of the evaporator and the condenser was slightly lower in winter when compared to the summer period. The lower temperature of the refrigerant at the inlet and the outlet of the heat exchangers during the winter period was partly responsible for the decrease in COPE when compared to its counterpart values during the summer period. The power consumed throughout the heating cycle, showed no significant difference among the different volumes of hot water drawn off and the average was 1.23 kW. The electrical energy consumed and the useful thermal energy gained demonstrated a significant difference between the 50 L drawn off (1.30 and 2.80 kWh) as opposed to the 100 or 150 L drawn off (1.89 and 4.18 kWh; 2.05 and 5.13 kWh). The average COPE for the different volumes of hot water drawn off was 2.30.

TABLE III. WINTER POWER, TEMPERATURES AND COPE WITH RESPECT TO SPECIFIC VOLUMES OF DRAWN OFF

Parameters	50 L drawn off recorded parameter values			100 L drawn off recorded parameter values			150 L drawn off recorded parameter values		
	Min	Max	Average	Min	Max	Average	Min	Max	Average
Tevpi / °C	-0.42	7.64	4.03	3.20	4.51	4.13	2.95	5.98	4.58
Tevpo / °C	12.22	28.81	19.64	16.01	23.13	19.12	19.38	30.77	24.08
Tconi / °C	62.60	77.33	69.15	66.79	72.77	69.92	69.91	79.71	74.12
Tcono / °C	37.22	42.52	39.79	36.66	37.85	37.35	34.83	39.03	36.69
p / kW	1.09	1.21	1.14	1.18	1.24	1.21	1.17	1.26	1.23
EE / kWh	1.21	1.45	1.30	1.65	1.87	1.75	1.89	2.15	2.05
TE / kWh	2.66	2.80	2.71	4.07	4.39	4.18	4.58	5.30	5.13
COPe	1.93	2.20	2.08	2.35	2.46	2.39	2.39	2.58	2.42

Tevpi = Refrigerant temperature at inlet of evaporator, Tevpo = Refrigerant temperature at outlet of evaporator, Tconi = Refrigerant temperature at inlet of condenser, Tcono = Refrigerant temperature at outlet of condenser, P = average power consumed, EE = Electrical energy consumed, TE = Thermal energy consumed, COPe = Energy dependent COP, Min = minimum, Max = maximum

*B. Thermodynamic COP and Impact of Refrigerant Pressures*

The refrigerant pressures and the enthalpies at the inlet and the outlet of the evaporator and the condenser and the derived coefficient of performance of the ASHP unit (COPT) were analysed for both the summer and winter periods under the 50, 100 and 150 L hot water drawn off.

*B1. Summer Performance of Refrigerant Pressures, Enthalpies and the COPT*

Table IV shows the minimum, the maximum and the average pressures and the enthalpies of the refrigerant at the inlet and the outlet of the evaporator and the condenser of the ASHP unit, together with the derived COPT during the VCRC, due to 50, 100 and 150 L of hot water drawn off. Table IV shows that, the average pressure of the refrigerant

at the inlet of the evaporator was 0.523 MPa and was practically equal to the average pressure of the refrigerant at the outlet of the evaporator (with an average of 0.513 MPa) in all the drawn off scenarios. The difference between the average enthalpy of the refrigerant at the outlet of the evaporator (395.33 kJ/kg) and the inlet of the evaporator (285.71 kJ/kg) was 109.62 kJ/kg. Therefore, it can be showed that thermal energy was gained by the refrigerant at the evaporator during the VCRC. The average pressure of the refrigerant at the inlet and the outlet of the condenser was practically equal to 2.70 MPa. The difference between the average enthalpy of the refrigerant at the inlet of the condenser (409.33 kJ/kg) and the outlet of the condenser (259.33 kJ/kg) was 150 kJ/kg. It can be depicted that thermal energy was dissipated from the refrigerant at the condenser during the VCRC. The average COPT for the different volumes of hot water drawn off was 3.52 and was higher than the corresponding COPe (3.02).

TABLE IV. SUMMER PRESSURE, ENTHALPY AND COPT WITH RESPECT TO SPECIFIC VOLUMES DRAWN OFF

Parameters	50 L Drawn off Recorded Parameter Values			100 L Drawn off Recorded Parameter Values			150 L Drawn off Recorded Parameter Values		
	Min	Max	Average	Min	Max	Average	Min	Max	Average
Pevpi / MPa	0.51	0.55	0.53	0.52	0.51	0.51	0.49	0.54	0.53
Pevpo / MPa	0.50	0.54	0.52	0.51	0.50	0.50	0.48	0.53	0.52
Pconi / MPa	2.06	2.98	2.68	2.68	2.74	2.68	2.46	3.10	2.76
Pcono / MPa	1.95	2.87	2.68	2.65	2.73	2.67	2.35	3.00	2.76
hevpi / kJ/kg	277.85	291.66	289.36	287.78	288.86	288.16	277.37	292.27	278.90
hevpo / kJ/kg	390.00	400.00	395.00	392.00	401.00	395.00	390.00	400.00	396.00
hconi / kJ/kg	405.00	420.00	410.00	405.00	415.00	410.00	400.00	420.00	408.00
hcono / kJ/kg	250.00	265.00	265.00	258.00	260.00	260.00	250.00	261.28	253.40
COPT	3.49	3.62	3.48	3.50	3.56	3.52	3.47	3.59	3.55

Pevpi = Refrigerant pressure at inlet of evaporator, Pevpo = Refrigerant pressure at outlet of evaporator, Pconi = Refrigerant pressure at inlet of condenser, Pcono = Refrigerant pressure at outlet of condenser, hevpi = Refrigerant enthalpy at inlet of evaporator, hevpo = Refrigerant enthalpy at outlet of evaporator, hconi = Refrigerant enthalpy at inlet of condenser, hcono = Refrigerant enthalpy at outlet of condenser, COPT = Thermodynamic COP, Min = minimum, Max = maximum

**B2. Winter Performance of Refrigerant Pressures, Enthalpies and the COPt**

Table V shows the minimum, the maximum and the average pressures and the enthalpies of the refrigerant at the inlet and the outlet of the evaporator and the condenser, and also, the derived COPt during the VCRC after 50, 100 and 150 L hot water drawn off. Table V depicted that the average pressure of the refrigerant at the inlet of the evaporator was 0.513 MPa, which was ideally equal to the average pressure of the refrigerant at the outlet of the evaporator (with an average of 0.516 MPa) with respect to the different volumes of hot water drawn off. The difference

between the average enthalpy of the refrigerant between the outlet of the evaporator (301.90 kJ/kg) and the inlet of the evaporator (252.79 kJ/kg) was 49.11 kJ/kg. The average pressure of the refrigerant at the inlet and the outlet of the condenser was equal (2.34 MPa). The difference between the average enthalpy of the refrigerant at the inlet of the condenser (393.70 kJ/kg) and the outlet of the condenser (253.65 kJ/kg) was 140 kJ/kg. It revealed that, there was absolute dissipation of the thermal energy from the refrigerant contained in the condenser during the VCRC. The average COPt of the ASHP unit for the different volumes of hot water drawn off was 2.65 and was higher than the corresponding COPE (2.23).

TABLE V. WINTER PRESSURE, ENTHALPY AND COPt WITH RESPECT TO SPECIFIC VOLUMES OF DRAWN OFF

Parameter	50 L Drawn off Recorded Parameter Values			100 L Drawn off Recorded Parameter Values			150 L Drawn off Recorded Parameter Values		
	Min	Max	Average	Min	Max	Average	Min	Max	Average
Pevpi / MPa	0.46	0.54	0.52	0.49	0.53	0.49	0.53	0.54	0.53
Pevpo / MPa	0.45	0.53	0.51	0.47	0.50	0.47	0.51	0.52	0.52
Pconi / MPa	2.16	2.58	2.25	2.11	2.41	2.25	2.25	3.10	2.51
Pcono / MPa	2.05	2.54	2.23	2.00	2.40	2.24	2.21	3.00	2.51
hevpi / kJ/kg	245.29	259.56	251.67	248.55	254.67	251.22	251.45	261.24	255.49
hevpo / kJ/kg	297.11	305.90	301.96	301.06	302.49	302.07	300.79	304.09	302.56
hconi / kJ/kg	390.76	394.90	394.34	393.11	394.11	394.11	385.72	387.72	392.65
hcono / kJ/kg	246.72	261.28	256.65	252.09	253.61	252.21	249.09	255.13	252.09
COPt	2.23	2.55	2.42	2.72	2.85	2.77	2.78	2.81	2.99

Pevpi = Refrigerant pressure at inlet of evaporator, Pevpo = Refrigerant pressure at outlet of evaporator, Pconi = Refrigerant pressure at inlet of condenser, Pcono = Refrigerant pressure at outlet of condenser, hevpi = Refrigerant enthalpy at inlet of evaporator, hevpo = Refrigerant enthalpy at outlet of evaporator, hconi = Refrigerant enthalpy at inlet of condenser, hcono = Refrigerant enthalpy at outlet of condenser, COPt = Thermodynamic COP, Min = minimum, Max = maximum

**C. Comparison of the COP of the ASHP Water Heater (COPE) and the COP of the ASHP Unit (COPt)**

A sample of the number of observations for corresponding COPE and COPt were compared in both summer and winter monitoring periods over the different volumes of hot water drawn off scenarios.

**C1. Comparison of the COPE and the COPt During the Summer Monitoring Period**

Figure 3 shows a plot of both COPE and COPt on the y-axis against the number of observations on the x-axis. It can be observed in Figure 3 that for identical observations from the sample, the COPt was higher when compared with the corresponding COPE. The average COPE and COPt for the samples of observations in Figure III was 3.04 and 3.53, respectively. The difference in the average COP between the COPt and COPE was 0.49. The higher values of the COPt may be possible due to the lesser input electrical energy consumed (energy consumed by the compressor

only) as opposed to the higher input electrical energy consumed (energy consumed by the compressor, fan and water circulation pump) in the case of the COPE.

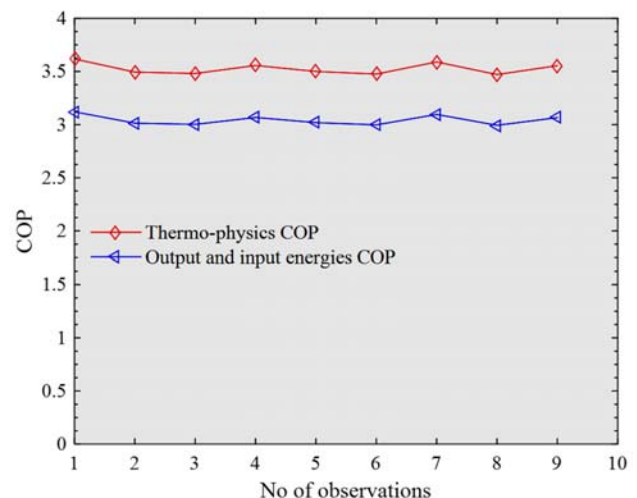


Figure 3. Comparison of the COPt and COPE for summer period

Nevertheless, the COP<sub>t</sub> can be further improved by the use of a refrigerant with exceptional thermo-physical properties.

The COP<sub>t</sub> can also be increased by the implementation of an efficient compressor, operating with a variable speed drive such that the power consumption will be able to varied with the heating loads during the VCRC. On the other hand, the COPE can be increased by the use of a high efficient fan, a water circulation pump and a compressor, which will employ variable speed drive, in their electric motors instead of the traditional induction motors.

### C2. Comparison of the COPE and COP<sub>t</sub> During Winter Monitoring Period

Figure IV shows a plot of both COPE and COP<sub>t</sub> on the y-axis against the number of observations on the x-axis. The average COPE and COP<sub>t</sub> for the samples of observations in Figure IV was 2.31 and 2.68, respectively. The difference in the average COP between the COP<sub>t</sub> and the COPE was 0.37. The average COP<sub>t</sub> was higher than the corresponding average COPE and the difference was significant. The difference between the COP<sub>t</sub> and COPE could be attributed to the additional input electrical power consumed by the water circulation pump and the fan in the case of the COPE, which contributed to 12.8% of the total power consumed by the ASHP water heater.

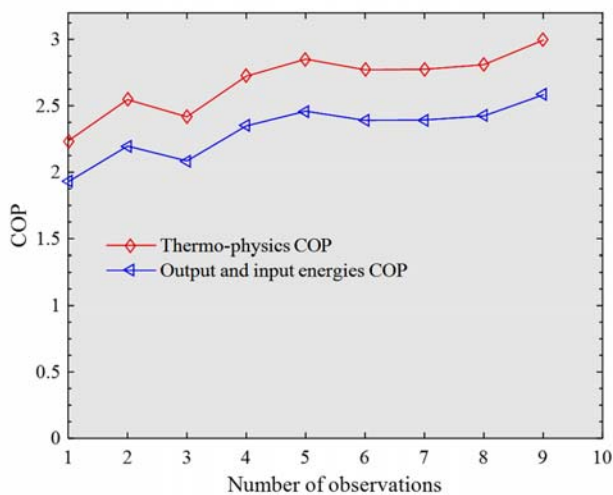


Figure 4. Comparison of the COP<sub>t</sub> and COPE for winter

## VI. CONCLUSIONS

We can conclude that the COP<sub>t</sub> of the ASHP unit was higher than the COPE of the ASHP water heater. The COP of the ASHP unit and the ASHP water heater depends strongly on the thermo-physical properties of the refrigerant and the design of the components that make up the VCRC. A potential implementation of efficient electric motors with variable speed drives to operate the compressor, water

circulation pump and the propeller axial fan of the ASHP water heater will enhance both the COPE and the COP<sub>t</sub>. Although, the performance of the ASHP water heater depends on the ambient temperature, the COP<sub>t</sub> will increase, if the enthalpy change of the refrigerant at the outlet and the inlet of the evaporator increases during the VCRC while the changed in enthalpy of the refrigerant at the inlet and the outlet of the condenser remain the same. It can be affirmed that there was a significant difference between the COP<sub>t</sub> and COPE. The input power consumed by the ASHP unit was 12.8 % lower than the input power consumed by the ASHP water heater. The corresponding change in enthalpy of the refrigerant at the condenser was greater than that at the evaporator throughout the different volumes of hot water drawn off. In conclusion, the COP of the ASHP water heater can be improved by ensuring that the COP during operation is almost equal to that of the ASHP unit. This could be achieved by using very efficient electric motors to drive the compressor, fan and the water circulation pump. And in addition, the electrical energy consumed by the fan and the water circulation pump should be negligible when compared to the electrical energy consumed by the compressor during the VCRC.

## ACKNOWLEDGMENT

We acknowledge Central University of Technology, research and postgraduate office for providing us funding which acted as an enabler for the execution of the research and the Faculty of Engineering, innovation and research committee for their financial assistance that helped us to purchase the research equipment.

## REFERENCES

- [1] Swan, L.G. and Ugursal, V.I., 2009. Modeling of end-use energy consumption in the residential sector: A review of modeling techniques. *Renewable and sustainable energy reviews*, 13(8), pp.1819-1835. <https://doi.org/10.1016/j.rser.2008.09.033>
- [2] Rousseau, P.G. and Greyvenstein, G.P., 2000. Enhancing the impact of heat pump water heaters in the South African commercial sector. *Energy*, 25(1), pp.51-70. DOI: 10.1016/S0360-5442(99)00053-5
- [3] Tangwe, S., Simon, M. and Meyer, E., 2014. Mathematical modeling and simulation application to visualize the performance of retrofit heat pump water heater under first hour heating rating. *Renewable energy*, 72, pp.203-211. DOI: 10.1016/j.renene.2014.07.011
- [4] Chua, K.J., Chou, S.K. and Yang, W.M., 2010. Advances in heat pump systems: A review. *Applied energy*, 87(12), pp.3611-3624. DOI: 10.1016/j.apenergy.2010.06.014
- [5] Hepbasli, A. and Kalinci, Y., 2009. A review of heat pump water heating systems. *Renewable and Sustainable Energy Reviews*, 13(6-7), pp.1211-1229. DOI: 10.1016/j.rser.2008.08.002
- [6] Morrison, G.L., Anderson, T. and Behnia, M., 2004. Seasonal performance rating of heat pump water heaters. *Solar Energy*, 76(1-3), pp.147-152. DOI: 10.1016/j.solener.2003.08.007
- [7] Bodzin, S., 1997. Air-to-water heat pumps for the home. *Home Energy*, 14(4).
- [8] Xu, G., Zhang, X. and Deng, S., 2006. A simulation study on the operating performance of a solar-air source heat pump water heater. *Applied Thermal Engineering*, 26(11-12), pp.1257-1265. 10.1016/j.applthermaleng.2005.10.033

[9] Peng, J.W., Li, H. and Zhang, C.L., 2016. Performance comparison of air-source heat pump water heater with different expansion devices. *Applied Thermal Engineering*, 99, pp.1190-1200. <https://doi.org/10.1016/j.applthermaleng.2016.01.113>

[10] Tangwe, S.L., Simon, M. and Mhundwa, R., 2018. The performance of split and integrated types air-source heat pump water heaters in South Africa. *Journal of Energy in Southern Africa*, 29(2), pp.12-20. <http://dx.doi.org/10.17159/2413-3051/2018/v29i2a4358>

[11] Kamel, R.S., Fung, A.S. and Dash, P.R., 2015. Solar systems and their integration with heat pumps: A review. *Energy and buildings*, 87, pp.395-412. <https://doi.org/10.1016/j.enbuild.2014.11.030>

[12] Staffell I, Brett D, Brandon N, Hawkes A. A review of domestic heat pumps. *Energy & Environmental Science*. 2012;5(11):9291-306. DOI: <http://dx.doi.org/10.1039/c2ee22653g>

[13] Vieira, A.S., Stewart, R.A. and Beal, C.D., 2015. Air source heat pump water heaters in residential buildings in Australia: Identification of key performance parameters. *Energy and buildings*, 91, pp.148-162. <https://doi.org/10.1016/j.enbuild.2015.01.041>

[14] Guo, X. and Goumba, A.P., 2018. Air source heat pump for domestic hot water supply: Performance comparison between individual and building scale installations. *Energy*, 164, pp.794-802. <https://doi.org/10.1016/j.energy.2018.09.065>

[15] Ashdown, B.G., 2004. Heat pump water heater technology: Experiences of residential consumers and utilities (No. ORNL/TM-2004/81). ORNL. DOI: 10.2172/885625

[16] Sinha, S.K. and Dysarkar, A., 2008. United States Patent Application: Heat Pump Liquid Heater. Available on <http://appft1.uspto.gov/netacgi/nphas on>, pp.19-04.

[17] Egbert B. and Rienk V.G, 2013. *Environmental Physics, sustainable energy and climate change*, 3rd Edition. A John Wiley & Sons, Ltd, Publication

[18] Peng, J.W., Li, H. and Zhang, C.L., 2016. Performance comparison of air-source heat pump water heater with different expansion devices. *Applied Thermal Engineering*, 99, pp.1190-1200. <https://doi.org/10.1016/j.applthermaleng.2016.01.113>

[19] Vieira, A.S., Stewart, R.A. and Beal, C.D., 2015. Air source heat pump water heaters in residential buildings in Australia: Identification of key performance parameters. *Energy and buildings*, 91, pp.148-162. <https://doi.org/10.1016/j.enbuild.2015.01.041>

[20] Lemmon, E.W., Huber, M.L. and McLinden, M.O., 2010. NIST Standard Reference Database 23, Reference Fluid Thermodynamic and Transport Properties (REFPROP), version 9.0, National Institute of Standards and Technology. R1234yf. fld file dated December, 22, p.2010.

[21] de Monte, F., 2002. Calculation of thermodynamic properties of R407C and R410A by the Martin-Hou equation of state—part II: technical interpretation. *International Journal of Refrigeration*, 25(3), pp.314-329. [https://doi.org/10.1016/S0140-7007\(01\)00028-7](https://doi.org/10.1016/S0140-7007(01)00028-7).

APPENDIX

Nomenclature	Full meaning
ASHP	Air Source Heat Pump
COP	Coefficient of performance
COPE	COP of ASHP water heater
COPT	COP of ASHP unit
EE	Electrical energy consumed in kWh
TE	Thermal energy gained in kWh
P	Average power consumed in kW
Pevpi	Refrigerant pressure at inlet of evaporator in MPa
Pevpo	Refrigerant pressure at outlet of evaporator in MPa
Pconi	Refrigerant pressure at inlet of condenser in MPa
Pcono	Refrigerant pressure at outlet of condenser in MPa
Tevpi	Refrigerant temperature at inlet of evaporator in oC
Tevpo	Refrigerant temperature at outlet of evaporator in oC
Tconi	Refrigerant temperature at inlet of condenser in oC
Tcono	Refrigerant temperature at outlet of condenser in oC
m	Mass of water heater in kg
c	Specific heat capacity of water in kJ/kg°C
Ti	Water temperature at inlet of ASHP
To	Water temperature at outlet of ASHP
VCRC	Vapour Compression Refrigeration Cycle

© 2020 Published by ECRES.